

We present a near-IR study of the EXor variable V1118 Ori, performed by following a slightly declining phase after a recent outburst. In particular, the near-IR (0.8 - 2.3 μm) spectrum, obtained for the first time, shows a large variety of emission features of the HI (Paschen and Brackett series), He I recombination and CO overtone. By comparing the observed spectrum with a wind model, a mass loss rate of $4 \cdot 10^{-8} M_{\odot} \text{ yr}^{-1}$ can be derived along with other parameters whose values are typical of an accreting T Tauri star. In addition, we have used X-ray data from the XMM archive, taken in two different epochs during the declining phase monitored in IR. X-ray emission (in the range 0.5 - 10 keV) permits to derive several parameters (as plasma temperatures and L_X luminosity) which confirm the T Tauri nature of the source. In the near-IR the object maintains a low extinction ($A_V \lesssim 2$) during all the activity phases, confirming that variable extinction does not contribute to brightness variations. The lack of both a significant amount of circumstellar material and any evidence of IR cooling from collimated jet/outflow driven by the source, indicates that, at least this member of the EXor class, is in a late stage of the Pre-Main Sequence evolution. Going from inactive to active phases the luminosity increases considerably (from $1.4 L_{\odot}$ to more than $25 L_{\odot}$) and the observed spectral energy distribution (SED) assumes different shapes, all typical of a T Tauri star. In the X-ray regime, an evident fading is present, detected in the post-outburst phase, that cannot be reconciled with the presence of any absorbing material. This circumstance, combined with the persistence (in the pre- and post-outburst phases) of a temperature component at about 10 MK, suggests that accretion has some influence in regulating the coronal activity.

Key words. stars: emission lines – stars: pre-main sequence – stars: variable – IR: stars – stars: individual: V1118 Ori – X-ray: stars

Evidence for T Tauri-like emission in the EXor V1118 Ori from near-IR and X-ray data ^{*}

D.Lorenzetti¹, T.Giannini¹, L.Calzoletti^{1,2}, S.Puccetti^{1,3}, S.Antoniucci^{1,3},
A.A.Arkharov⁴, A.Di Paola¹, V.M.Larionov⁵ and B.Nisini¹

¹ INAF - Osservatorio Astronomico di Roma, via Frascati 33, I-00040 Monte Porzio (Italy)

² Università degli Studi di Cagliari - Dipartimento di Fisica, S.P. Monserrato-Sestu Km 0.700, I-09042 Monserrato-CA (Italy)

³ Università degli Studi di Roma "Tor Vergata" - Dipartimento di Fisica, via della Ricerca Scientifica 1, I-00133 Roma (Italy)

⁴ Central Astronomical Observatory of Pulkovo, Pulkovskoe shosse 65, 196140 St.Petersburg, Russia

⁵ Astronomical Institute of St.Petersburg University, Russia

e-mail: dloren,giannini,calzol,puccetti,antoniucci,dipaola,nisini@mporzio.astro.it; arkharov@mail.ru; vm1@VL1104.spb.edu

Received;Accepted

Abstract.

1. Introduction

The star V1118 Ori is considered a pre-main sequence EXor variable which undergoes subsequent outbursts in optical light. The EXors class (whose name derives from the prototype EX Lup) is composed by nine members defined and listed by Herbig (1989). These sources are phenomenologically characterized by repetitive outbursts with an amplitude of up to 5 magnitudes, lasting one year or less, with a recurrence time of about 5-10 years. They are supposed to live an intermediate phase between the strong FUor eruptions and the more quiescent main sequence (Herbig 1977, Hartmann, Kenyon & Hartigan 1993), during which they exhibit an activity level lower than the FUors one. The differences between FUor and EXor outburst are not so evident in intensity, since both classes have comparable outburst amplitudes, but in duration, remaining the former bright for decades and the latter only for months. Indeed, whether the EXor evolutionary

Send offprint requests to: Dario Lorenzetti, email:dloren@mporzio.astro.it

^{*} Based on observations collected at the AZT-24 telescope (Campo Imperatore, Italy)

stage follows the FUor one, or merely represents a less evident manifestation attributable to the same phase, is a matter not yet completely ascertained. As for the FUor analogs, the EXor outbursts are believed to arise from enhanced accretion events from a circumstellar disk, although associated with lesser values of the mass accretion rate (\dot{M}). The quite uncertain picture which emerges in interpreting the EXors phenomenon stems from the small number of known objects and from the lack of a long-term multi-frequency monitoring of the photometric and spectroscopic properties.

By examining the case of the eruptive object V1118 Ori, four outbursts have been observed so far, although archival plates suggest that there were further flares in the past (1939-1956 - Paul et al. 1995). The first documented burst was during the period 1982-1984 (Chanal 1983; Parsamian & Gasparian 1987); the second in 1988-1990 (Parsamian et al. 1993); the third in 1992-1994 (García García et al. 1995); the fourth in 1997-1998 (Hayakawa et al. 1998; García García & Parsamian 2000). The last outburst at the end of 2004 was announced by Williams & Heathcote (2005) and currently (September 2005), the object is slowly fading but has not yet reached its quiescent phase. Typically, the amplitude of the outburst (in V band) is larger than 3 magnitudes (from about 17-18 to 14.5) and the duration is longer than 2 year, with a rise time of 8-10 months followed by a long-lived decline phase of about 1.5 years. An optical spectrum (from 3900 to 5600 Å) was obtained (Gasparian et al. 1990) during the rising period of the second outburst in the early 1989. It shows emission lines of H I, Ca II, Fe I and Fe II and the presence of P-Cyg profiles in the Balmer series is suspected: this spectrum is similar to that of T Tauri stars with moderate intensity. Prior to the most recent outburst, the source was photometrically observed at near infrared wavelengths only three times during both outburst and quiescence phases. We present here the first near IR spectrum of V1118 Ori along with broad and narrow band imaging data obtained during the last declining phase. A newly obtained X-ray detection during the same phase is presented as a result of a search in the existing archives. Accretion processes have been suggested as the possible origin of the X-ray emission of young low mass objects (e.g. Shu et al. 1997). However the mechanisms are still unclear since many of these objects emit X-rays via solar-like magnetically trapped coronal plasma (see the review by Feigelson & Montmerle 1999; Kastner et al. 2004a).

Archival X-ray data come from a multi-wavelength campaign to monitor the 2004/2005 outburst of V1118 Ori. Such monitoring is conducted by Audard et al. (2005), who have very recently presented their first results. They focus mainly on the X-ray properties, although accurately sampled optical and IR light curves are presented, as well. They argue that the X-ray emission was due to a corona, but it was influenced by the accretion during the outburst. Their time coverage partially overlaps with our early observations which, however, complement their results by covering a subsequent period, relevant to ascertain the source behaviour.

The IR study carried out during the declining/quiescent phase allows us to investigate how the properties of the circumstellar matter prior the outburst will influence, through the accretion, the outburst itself. The same study during the active phase samples how the circumstellar material is altered by intermittent mass loss. The X-ray investigation carried out during an optical/near IR monitoring can help in discriminating between the mechanism(s) which generate(s) the high energy emission in low mass protostars. Our aim is manifold: (i) to better understand how the IR spectral signatures are related to the intrinsic nature of an EXor; (ii) to derive a consistent picture for both the IR and X-ray behaviour; and (iii) to build up a systematic IR database useful as a reference for the next monitoring of the quiescence and subsequent outburst phases. After a short presentation in Sect.2 of our observations and data reduction procedures, we provide and discuss the results in Sect.3, giving our conclusions in Sect.4.

2. Observations and data reduction

2.1. Near IR imaging and spectroscopy

Near IR data were obtained at the 1.1m AZT-24 telescope located at Campo Imperatore (L'Aquila - Italy) equipped with the imager/spectrometer SWIRCAM (D'Alessio et al. 2000) which is based on a 256×256 HgCdTe PICNIC array. Photometry is performed with broad band filters J ($1.25 \mu\text{m}$), H ($1.65 \mu\text{m}$) and K ($2.20 \mu\text{m}$) along with a narrow band one, centered at $2.122 \mu\text{m}$ on the 1-0 S(1) H_2 transition. The total field of view is 4.4×4.4 arcmin² which corresponds to a plate scale of 1.04 arcsec/pixel. Low resolution ($\mathcal{R} \sim 250$) spectroscopy is obtained by means of two IR grisms G_{blue} and G_{red} covering the ZJ ($0.83 - 1.34 \mu\text{m}$) and HK ($1.44 - 2.35 \mu\text{m}$) bands, respectively, in two subsequent exposures. The long slit is not orientable in position angle and samples a pre-defined portion of the focal plane, 2×260 arcsec along the east-west direction. Details of the observations are given in Table 1. All the observations were obtained by dithering the telescope around the pointed position. The raw imaging data were reduced by using standard procedures for bad pixel removal, flat fielding and sky subtraction. Continuum-free images in the narrow band filter were obtained as a first step by subtracting an appropriately scaled K image from the H_2 image. Such scaling has been obtained by performing the photometry of a number of stars located in different positions within the field.

Long slit spectroscopy was carried out in the standard ABB'A' mode with a total integration time of 800 sec. The observations were flat fielded, sky subtracted and corrected for the optical distortion along both the spatial and spectral direction. Telluric features were removed by dividing the extracted spectra by that of a normalized telluric standard star, once corrected for its intrinsic spectral features. Wavelength calibration was derived from OH lines present in the raw spectral images, while flux calibration was obtained from our photometric data.

Table 1. Journal of observations

UT Date	MJD ^a	Mode	Filter/Grism
Mar 20, 05	53449	Phot	J,K
Apr 03, 05	53463	Phot	J,K
Apr 15, 05	53475	Phot	J,K
Sep 06, 05	53619	Phot	J,K, H ₂
Sep 11, 05	53624	Phot/Spec	JHK, G _b ,G _r

Notes to the Table:

a - MJD = modified Julian Date.

2.2. X-ray observations

Aiming to obtain reliable X-ray data on V1118 Ori, we searched the public archives, finding the XMM-Newton results of pointed observations taken during our monitoring period. The relevant information on both the X-ray telescope and EPIC (PN and MOS) cameras are given by Jansen et al. (2001), Strüder et al. (2001) and Turner et al. (2001), respectively. Table 2 summarizes the two XMM-Newton available observations. The first was obtained few months after the most recent outburst (see also Audard et al. 2005), while the second (on Sept. 08, 2005), obtained 7 months later, is almost simultaneous with our near IR spectrum, taken 3 days after. The data have been processed using the XMM-Newton Science Analysis Survey (SAS) v.6.1.0. We used the event files linearized with a standard reduction pipeline (Pipeline Processing System, PPS) at the Survey Science Center (SSC, University of Leicester, UK).

Events spread at most in two contiguous pixels for PN (i.e. pattern=0-4) and in four contiguous pixels for MOS (i.e. pattern=0-12) have been selected. Event files were cleaned from bad pixels (hot pixels, events out of the field of view, etc.) and the soft proton flares.

In order to remove periods of unwanted high background level, we located the flares by analyzing the light curves of the count rate at energies higher than 10 keV, where the X-ray sources contribution is negligible. We rejected the time intervals, when the count rate is higher than 11 (8 for 0212481101 observation) counts s⁻¹ and 1.3 counts s⁻¹ for the PN and MOS cameras respectively. The source counts were extracted from a circular region of 25 arcsec radius. The background counts were extracted from the nearest source free region. The response and ancillary files were generated by the XMM-SAS tasks, RMFGEN and ARFGEN, respectively. The MOS1 and MOS2 spectra are combined together. The spectra are binned to have at least 20 counts per energy bin.

Table 2. X-ray detections parameters

obs.id.	UT Date	MJD ^a	EPIC	t_{int}	(counts s ⁻¹) ^b	
			cam	(sec)	(0.5-10 keV)	(0.5-2 keV)
0212480301	Feb 18, 05	53419	PN/MOS	1.7 10 ⁴	0.0162	0.0132
0212481101	Sep 08, 05	53621	PN	1.3 10 ⁴	0.0044	0.0027

Notes to the Table:

a - MJD = modified Julian Date.

b - counts are for the PN camera and are background subtracted.

Table 3. Near IR photometry of V1118 Ori

MJD ^a	J	H	K	J-H	H-K
48260-49350 ^b	12.21 (1)	11.29 (1)	10.49 (1)	0.92	0.80
49426 ^c	8.52 (5)	8.04 (4)	7.94 (3)	0.48	0.10
51872 ^d	12.64 (2)	11.51 (3)	10.85 (2)	1.13	0.66
53449	11.16 ^e	-	9.79	-	-
53463	10.79	-	9.48	-	-
53475	10.94	-	9.53	-	-
53619	11.08	-	9.71	-	-
53624	11.23	10.45	9.85	0.78	0.60

Notes to the Table:

a - MJD = modified Julian Date.

b - The authors (Hillenbrand et al. 1998) do not specify the date of the observation which was taken during the period 1991-1993. The errors (in units of 0.01 mag) are given in parentheses.

c - Data from García, García et al. (1995).

d - 2MASS observation.

e - Errors of our photometry in all the three bands never exceed 0.02 mag.

3. Results and discussion

3.1. Near IR Imaging and Photometry

In Table 3 the photometric data are presented. For the sake of completeness, we report in the first three lines of Table 3 the near IR photometric data available in literature prior to the recent outburst. The maximum brightness corresponds to the third outburst active phase (García García et al. 1995) and the minimum to the most recent quiescent phase (2MASS All-Sky Catalog of Point Sources - Cutri et al. 2003): the J,H and K

brightness decreases by 4.1, 3.5 and 2.9 mag, respectively, thus less and less pronounced variations occur, while the wavelength increases. The third available near IR observation (Hillenbrand et al. 1998) was obtained during an almost quiescent phase and is in agreement with the described trend. Our results (from the fourth to the last line of Table 3), are sampling the slow declining after the recent outburst and substantially agree with the results of Audard et al. (2005). Since the data given in Table 3 refer to different outburst and quiescence phases and are not taken simultaneously with the optical data collected from the literature, they cannot be used, in principle, to construct any significant SED. However, we can assume that maxima and minima of different epochs recur at similar flux levels, a circumstance which is reasonably confirmed by the past record of optical observations. Under this hypothesis we plot in Figure 1 two SEDs, obtained by considering the weakest and the strongest values, respectively. To enlarge as much as possible the SED frequency range, we searched the IR archives (IRAS, ISO, MSX) for a mid- far-infrared counterpart of V1118 Ori and we were able to detect a faint emission (at a 2σ level) from a point-like source only in the MSX A-band at $8.28 \mu\text{m}$ which corresponds to a flux density of 0.3 Jy, obtained during a quiescent phase. This value suffers from a certain degree of contamination, of about 30 %, which is not due to the nearby bright star V372 Ori, but to the irregular diffuse emission characteristic of this sky area. In the MSX C-band (at $12.13 \mu\text{m}$) only an upper limit of 0.5 Jy, corresponding to the closeby sky emission, can be derived. This MSX determination, although marginal, is quite important since permits both to delineate the SED shape from the U band to the mid-IR and to compute a reliable value of the bolometric luminosity (L_{bol}). The MSX detection has been obtained during an inactive phase (July 1996), and, as such, it has to be attributed only to the quiescent SED. We lack of mid-IR detection during an active phase, however the source is expected to increase its brightness at all wavelengths, as proven by Muzerolle et al. (2005). In fact, they revealed the outburst of V1647 Ori (whose EXor or FUor nature is still not ascertained) with *Spitzer Space Telescope*, reporting a brightening in all the $3.6\text{-}70 \mu\text{m}$ range. By integrating the flux densities, we obtain L_{bol} values of 1.4 (quiescence) and 25.4 (outburst) L_{\odot} , respectively. The latter has to be considered as a lower limit, since in the L_{bol} (outburst) computation we used the same flux at $8.28 \mu\text{m}$ ascribed to the inactive phase. These values indicate how the increase in brightness is indeed impressive, a factor of more than 18, and suggest that the V1118 Ori luminosity ($< 10 L_{\odot}$) is more typical of the EXors than the 5-50 times more luminous FUors.

The SEDs reported in Figure 1 present different shapes: more peaked in the near infrared, looking like the T Tauri averaged SED (D’Alessio et al. 1999), or rather flat which resembles that typical of the eruptive objects (FUors-EXors) (Kóspál et al. 2004, Muzerolle et al. 2005). All these shapes are characteristic of accreting T Tauri stars which show indeed variable SEDs in IR. The apparent steepening of the SED during the out-

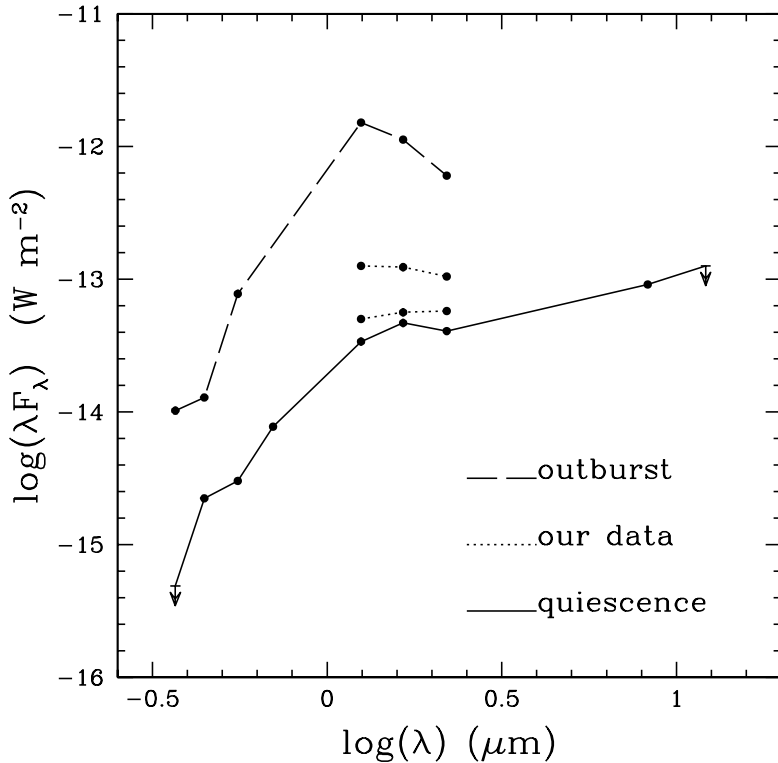


Fig. 1. Observed SEDs of V1118 Ori constructed with literature and present paper IR data that correspond to different activity phases as indicated in the bottom right corner.

burst is due to a single JHK photometry and, as such, does not necessarily apply to all the outburst phases. Based on JHK data plotted by Audard et al. (2005), a systematic variation of the SED slope with the activity phase does not seem recognizable. A systematic IR monitoring of repeated outbursts has to be accumulated to ascertain whether or not the SED is flattening while the source is progressively fading.

The same aspect can be furtherly discussed by following as the source behaves in the [J-H], [H-K] two colours diagram given in Figure 2. The locations of V1118 Ori as detected in epochs of different level of activity, indicate how the colours are well in agreement with those predicted for T Tauri stars by Meyer, Calvet & Hillenbrand (1997). Such predictions result from disk models with a range of accretion rates, inner disk radii and viewing angles. We remark how the observed data are largely consistent with unreddened values, implying that in the majority of the cases the object is seen practically through a negligible extinction ($A_V \simeq 0$). In one phase, far from the outburst, it appears slightly redder and the same happens in the optical band, as well. The very similar case of outburst recently studied over a large range of frequencies, namely V1647

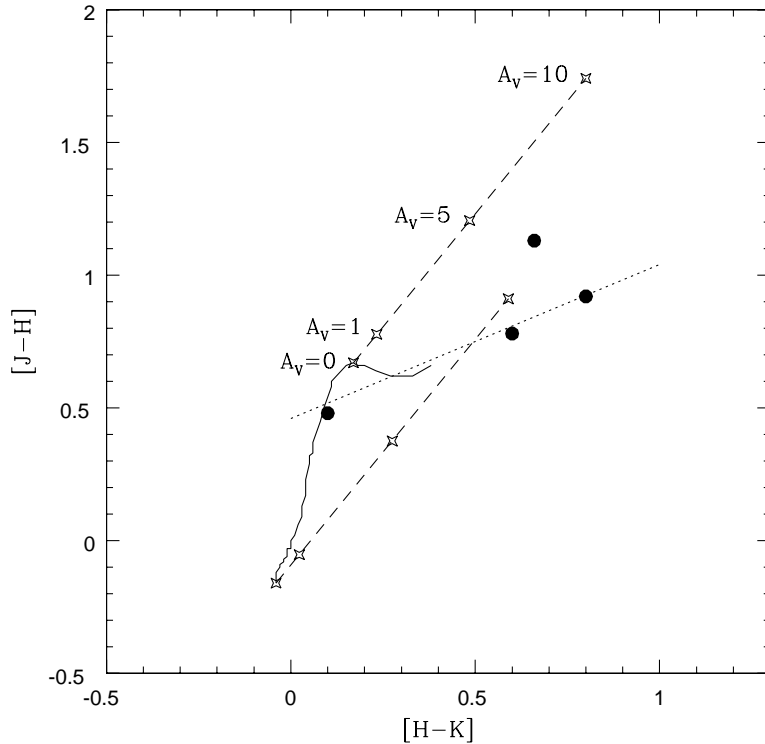


Fig. 2. Locations of V1118 Ori on a near IR two colours diagram in different epochs. The solid line marks the unreddened Main Sequence, whereas the dotted one the locus pertaining to the T Tauri stars (Meyer et al. 1997). Dashed lines are the reddening law according to Rieke & Lebofsky (1985); 10 mag intervals of A_V are indicated by crosses.

Ori, behaves exactly in the same manner as V1118 Ori in the near IR (Reipurth & Aspin 2004; Vacca et al. 2004). With reference to Figure 2 the observed shift in colours is compatible with an extinction value of $A_V \sim 2$ mag. Variable scattering by some cavity walls might contribute in making bluer the emerging light.

Several comparison stars are available within the $4'.4$ SWIRCAM field; in particular one of them has remained stable within 0.01 mag in JHK during our entire monitoring period, thus it is used to construct the near IR light curves in terms of differential photometry. A slightly downward trend is superposed on statistically meaningful variations (of about 0.2-0.3 mag) in the near IR on a shorter time scale (days). Such rapid variations detected in all the JHK bands do not seem related to extinction variability which should determine larger peak to peak variations at shorter wavelengths. This circumstance provides support to the idea that accretion processes are dynamical on several timescales: non steady accretion and rotational modulations occur from hours to weeks, while insta-

bilities of the magneto-spherical structure and EXors-FUors events are characterized by longer timescales (months to years).

Our H₂ image at 2.122 μm shows no presence of any emission down to a level of $1.1 \cdot 10^{-14} \text{ erg s}^{-1} \text{ cm}^{-2}$ (at 3σ) within a $4.4 \times 4.4 \text{ arcmin}^2$ FoV. The 1-0 S(1) H₂ line at 2.122 μm is one of the best tracer of the gas cooling after the passage of a shock front typically associated to jet structures emerging from a central object. Our sensitivity in revealing knots of H₂ emission ($L_{H_2} = 7 \cdot 10^{-5} L_{\odot}$) would have allowed us to detect the faintest knots and jets discovered by Stanke et al. (2002) during their unbiased H₂ survey of Orion. No other IR spectral features indicative of shock cooling (e.g. [Fe II] at 1.25 or 1.64 μm) are detected in our spectrum (see below, Sect. 3.2). Although the presence of an optical jet cannot be excluded, our observation agrees with the lack of collimated jets. This is a quite common feature in EXor and FUor objects that usually show powerful mass loss only in form of isotropic winds.

3.2. Near IR Spectroscopy

During the recent slowly declining phase we have obtained the first near-IR spectrum of V1118 Ori depicted in Figure 3 (see also Di Paola et al. 2005). The derived line fluxes are given in Table 4. It is an emission line spectrum dominated by the hydrogen recombination (Brackett and Paschen series) which signals the presence of ionized gas close to the star. Our spectral resolution does not allow to reveal whether lines have P Cygni profiles. We also detect Mg I line emission at 1.503 μm, weaker emission features of He I and a marginal (at $S/N = 2$) emission of Na I at 2.208 μm. These atomic features are commonly found in the near-IR spectra of T Tauri stars and younger objects. In particular, Mg I and Na I emission lines have been recently revealed in another erupting object, namely V1647 Ori (Reipurth & Aspin 2004; Vacca, Cushing & Simon 2004), where, however, He I is present in absorption. We note that Na I line has been also detected, but in absorption, (Herbig et al. 2001), in the near-IR spectrum of EX Lup, the prototype of the EXor class. These circumstances suggest that an IR spectroscopic data-base of eruptive variables, large enough to cover different activity phases, has to be built up in order to evaluate how possible similarities among EXors can be related to the dominant mechanism(s) of gas excitation and cooling. Molecular hydrogen contributions are absent and only the 1-0 S(1) rovibrational line at 2.122 μm is marginally recognizable at a 1σ level; such a spectroscopic circumstance confirms the lack of any shock evidence also indicated by H₂ imaging (Sect.3.1). The observed spectrum is much more similar to that of an accreting T Tauri star (Greene & Lada 1996) than the FUor ones. All these latter, apart a couple of exceptions, have spectra always dominated by absorption lines (Reipurth & Aspin 1997).

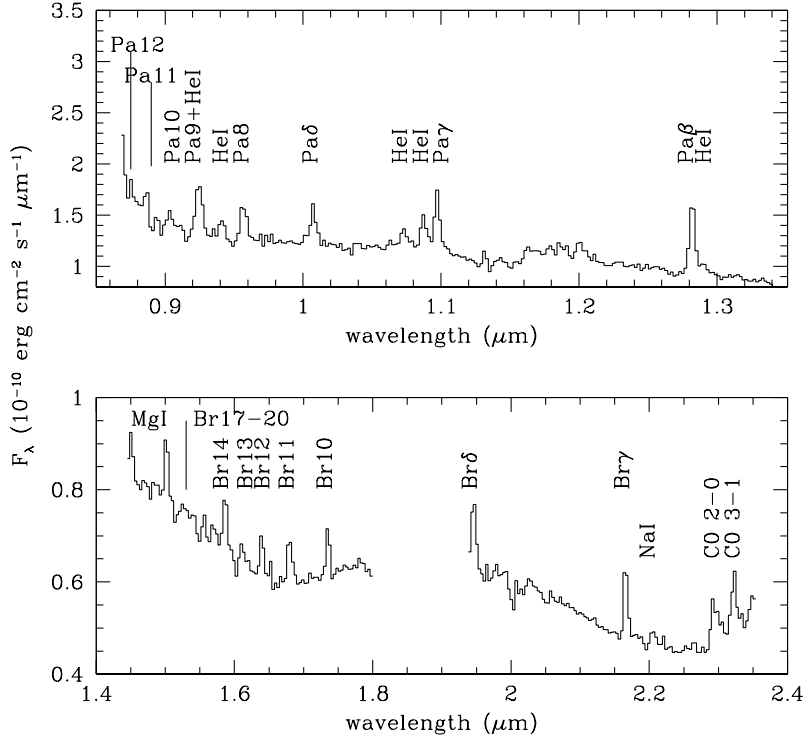


Fig. 3. Near-IR spectrum of V1118 Ori. The lines Pa 11 and Pa 12 are identified here, but are neither listed in Table 4 nor used in our model, since their fluxes suffer large uncertainties due to the definition of a reliable local baseline.

We have checked that no contamination exists due to the HII region associated to the nearby bright star V372 Ori. In Table 4 the identified lines along with the measured fluxes are given. The associated uncertainty refers to the rms of the local baseline.

The CO overtone emission $v=2-0$, $v=3-1$ is clearly detected; the same occurs in several young stellar objects (Carr 1989), although in the majority of FUor CO bands are revealed in absorption (Hartmann, Hinkle & Calvet 2004). In all the cases CO emission is seen together to Br γ line emission, but the two features likely come from different volume of gas. At temperatures of about 4000 K CO is dissociated and for values greater than 3000 K molecular hydrogen is dissociated by collisions. However, for density values greater than 10^7 cm^{-3} and in presence of H_2 , CO dominates the cooling (Scoville et al. 1980). Therefore the CO bands are specific probes of the circumstellar portions where the gas is relatively warm at high densities. Carr (1989) has quantitatively investigated two scenarios which account for the observed CO emission: an accretion disk and a neutral stellar wind with velocities of $100\text{-}300 \text{ km s}^{-1}$, where the gas is assumed to be cool ($\sim 3000 \text{ K}$). In this latter case, which agrees with our observations (see below this section), he

Table 4. Line emission fluxes of V1118 Ori

λ_{vac} (μm)	Ident.	$F \pm \Delta F$ ($10^{-13} \text{ erg s}^{-1} \text{ cm}^{-2}$)
0.9017	Pa10	1.6 ± 0.1
0.9230	He I	0.8 ± 0.1
0.9231	Pa9	3.1 ± 0.1
0.9548	Pa8	2.3 ± 0.2
1.0052	Pa δ	2.2 ± 0.2
1.0670	He I	1.2 ± 0.3
1.0832	He I	1.9 ± 0.2
1.0941	Pa γ	2.5 ± 0.2
1.2822	Pa β	4.1 ± 0.1
1.2850	He I	1.0 ± 0.1
1.5031	Mg I	0.8 ± 0.2
1.5885	Br14	0.8 ± 0.2
1.6114	Br13	0.5 ± 0.2
1.6412	Br12	0.6 ± 0.2
1.6811	Br11	0.9 ± 0.3
1.7367	Br10	0.8 ± 0.2
1.9451	Br δ	1.0 ± 0.2
2.1661	Br γ	1.2 ± 0.2
2.2084	Na I	0.4 ± 0.2
2.2935	CO 2-0	1.2 ± 0.4
2.3227	CO 3-1	1.3 ± 0.3

provides model predictions for deriving the mass loss rate from the CO (2-0) luminosity (his Figure 8). The CO flux, calculated in the 2-0 band by integrating from 2.29 and 2.32 μm after continuum subtraction, provides a CO luminosity L_{CO} equal to $6.3 \cdot 10^{-5} L_{\odot}$ and consequently a mass loss value in the range $(3-8) \cdot 10^{-7} M_{\odot} \text{ yr}^{-1}$ can be derived. The uncertainty range accounts for the varying model parameters.

The observed HI line emission has been compared with a wind model (Nisini, Antonucci & Giannini 2004) which considers a spherically symmetric and partially ionized envelope with a constant rate of mass loss ($\dot{M} = 4\pi r^2 \rho(r)v(r)$). The emitting gas is assumed to be in LTE and the adopted gas velocity law is:

$$v(r) = v_i + (v_{max} - v_i)[1 - (R_*/R)^\alpha] \quad (1)$$

where v_i and v_{max} are the initial and maximum wind velocity, respectively, while R_* is the stellar radius. The best fit to the data points is obtained for the following set of parameters: gas temperature of 10^4 K, $v_i = 20 \text{ km s}^{-1}$, $v_{max} = 200 \text{ km s}^{-1}$, envelope

internal radius $R_i = 1 R_*$, envelope thickness equal to $8 R_*$, mass loss rate $\dot{M} = 4 \cdot 10^{-8} M_\odot \text{ yr}^{-1}$. An important parameter of the model is the extinction value (A_V) for which the line fluxes need to be corrected. From analyzing the position of the object in the two colours diagram (Sect.3.1), we have assumed $A_V = 0$, a value well consistent with our observations. Figure 4 shows the line ratios of the Brackett and Paschen series with respect to the $\text{Br}\gamma$ and $\text{Pa}\beta$, respectively, along with the best fit model, whose parameters are indicated, as well. In addition, the model predicts for the $\text{Br}\gamma$ a flux of $1.3 \cdot 10^{-13} \text{ erg s}^{-1} \text{ cm}^{-2}$, practically equal to the observed one ($1.2 \cdot 10^{-13} \text{ erg s}^{-1} \text{ cm}^{-2}$, see Table 4). The effects of introducing a different extinction value ($A_V = 2$, namely the maximum allowed by the observations) are also depicted in Figure 4.

Finally, by ratioing the mass loss rates derived respectively from the HI recombination ($4 \cdot 10^{-8} M_\odot \text{ yr}^{-1}$) and the CO emission ($(3-8) \cdot 10^{-7} M_\odot \text{ yr}^{-1}$), a ionization fraction of about 0.1-0.2 can be derived. This value is largely consistent with those typical of active T Tauri environments (Greene & Lada 1996).

Aiming to evaluate the uncertainties on the derived parameters and to check the sensitivity of our model, we have computed the range of variation for each input parameter that is allowed to eventually provide line flux predictions comparable (within a 50 % extent) with the observed values. Such analysis indicates that gas temperature is one of the less sensitive parameters: variations between 5000 K and 15000 K do not affect the fit significantly. Conversely, other parameters are quite critical and their variability ranges are consequently rather narrow; we obtain: $\dot{M} = 4 \pm 2 \cdot 10^{-8} M_\odot \text{ yr}^{-1}$, $R_i = 1 - 2 R_*$, thickness $8 \pm \frac{4}{2} R_*$. Finally we note that no realistic solution can be found by using $A_V = 2$ mag: indeed this would imply an \dot{M} increase of about 50 % and a predicted $\text{Br}\gamma$ flux exceeding the observed value by more than one order of magnitude.

3.3. X-ray properties

The XMM data were modeled using the XSPEC spectral analysis package. The first observation (see Table 2), was firstly fitted over the 0.5 to 10 keV range with an almost unabsorbed two temperatures MEKAL thermal model (Mewe et al. 1995), which minimizes the χ^2 . The solar metal abundance has been adopted for Orion (Esteban et al. 1998), however, a trial with a value half than solar provided no significant improvement in the χ^2 value. In Figure 5 (*top panel*) a comparison between the observed spectra with the best fit model is given. The derived parameters, are given in the first line of Table 5. By looking at the fit, the suspicion could arise that a background contamination affects the data at energies greater than 3-4 keV. Therefore, as a second attempt, we fitted only the data points up to 3.5 keV. Following the analysis done by Audard et al (2005), we fitted these (2005 February) data with a single temperature, obtaining the result given in Figure 5 (*middle panel*), along with the parameters reported in the second line of

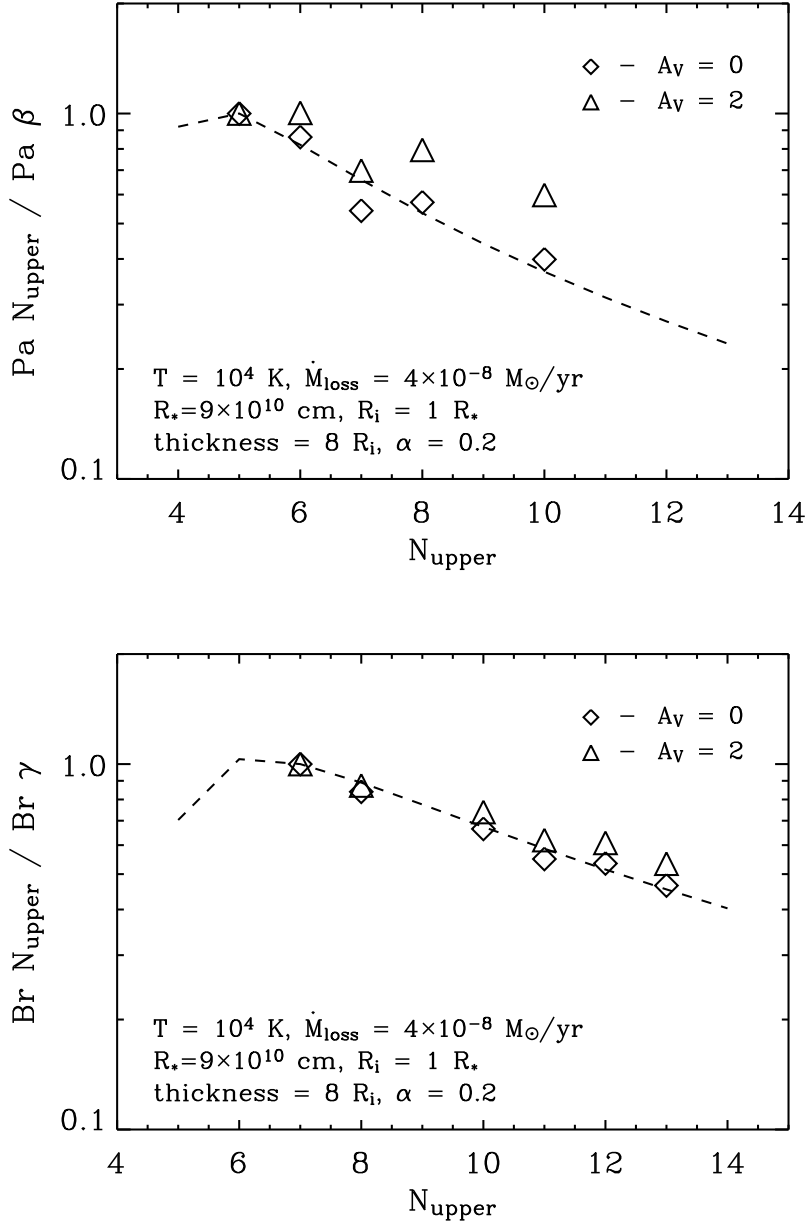


Fig. 4. *Top Panel:* Line ratios of the Paschen series with respect to the $\text{Pa}\beta$ line. Diamonds and triangles refer to our observations underdreddened ($A_V = 0$) and extinction corrected ($A_V = 2$), respectively. The dashed line represents the model line ratios. The relevant fit parameters are reported at the top of the panel. *Bottom Panel:* the same, but line ratios refer to the Brackett series with respect to the $\text{Br}\gamma$ line.

Table 5; such parameters substantially agree with the Audard et al. results. We also investigated the possibility to fit the data with a two temperatures model obtaining the result plotted in Figure 5 (*bottom panel*), and the parameters given in the third line of Table 5. The two temperature fit is as much acceptable as the single temperature (see the residuals behaviour in Figure 5 (*bottom panel*)) and has a N_H value which better

agrees with a rather unobscured line of sight. The circumstance that a good fit can be obtained with two temperature values (about 30 and 7 MK), similar to those able to account for the X-ray emission as detected prior the outburst (Audard et al. 2005), confirms that X-ray emission of V1118 Ori is practically unaffected by accretion events, being originated in the corona. Thus, the eventual disappearance of a high temperature component of the coronal emission, should occur with a certain delay with respect to the outburst. The second spectrum reported in Table 2 was obtained in Sept. 2005 (i.e. seven months later). Although this latter X-ray spectrum is integrated as long as the former, it appears intrinsically weaker and a decent fit can be obtained only with a single temperature (of about 10 MK) and by leaving the absorbing column density (N_H) as a free parameter (fourth line of Table 5). However, the best fit value, corresponding to a visible extinction $A_V < 2$ (see Table 5) is consistent with that of the earlier observation ($A_V = 1$). This fact is quite important since it proves that the X-ray fading is real and not due to any intervening extinction effect. Remember that also the near IR spectrum, taken in coincidental simultaneity (just 3 days later), could be fitted only by assuming $A_V \simeq 0$. The small difference between the extinction value derived from the X-ray measurement by assuming a gas-to-dust ratio typical of the interstellar medium and that derived from the simultaneously taken near IR spectrum, confirms the suggestion that the gas-to-dust ratio nearby the young stars could be larger than interstellar (Kastner et al. 2004b). The Sept. 2005 observation corresponds to L_X (0.5-3.5 keV) = $0.6 \cdot 10^{-4} L_\odot$ = $2.7 \cdot 10^{29}$ erg s $^{-1}$; assuming that the true stellar luminosity ranges between 0.5 and 1 L_\odot , then $\text{Log}(L_X/L_{bol}) > -4.2$, namely the star is much more active than our Sun (for which $\text{Log}(L_X/L_{bol}) \sim -6.5$).

By examining the data in Table 5, we remark: *i*) a real fading of about a factor of 4 is occurred in the X-ray emission (0.5 - 3.5 keV) between February and September 2005; *ii*) the existence of a temperature component, of about 7 MK, during the active phases, interpreted as a coronal signature (Audard et al. 2005) is a persistent feature even in the post outburst phase, while the X-ray emission of the object begins to decline. Recently, Preibisch et al. (2005), have presented their survey (named COUP) of nearly 600 X-ray emitting T Tauri stars in Orion and interpreted the widespread existence of a common temperature around 10 MK, or less, as a real feature of the coronal temperature distribution. Our data are fully in agreement with their findings, confirming the active T Tauri nature of V1118 Ori. Attributing to the coronal activity the fairly constant temperature component, detected even at a lower level of X-ray emission, is in contrast with the interpretation given by Grosso et al. (2005) of the recent eruption of V1647 Ori (Kastner et al. 2004b); however, the inconsistencies pertaining to the long standing debate on the dominant X-ray mechanism in YSO, are discussed by Audard et al. (2005).

The detected fading could be interpreted in the context of the magnetically active stars that show a significant X-rays variability (e.g. Feigelson & Montmerle 1999), but its

Table 5. X-ray derived parameters

UT Date	χ^2	d.o.f	N_H (10^{22} cm^{-2})	kT ₁ (keV)	kT ₂ (keV)	EM ₁ ^a (10^{52} cm^{-3})	EM ₂ ^a (10^{52} cm^{-3})	Flux ($10^{-14} \text{ erg s}^{-1} \text{ cm}^{-2}$) (0.5-10 keV)	(0.5-3.5 keV)
Feb 18, 05	35.7	35	0.19 ^b	$2.8 \pm_{1.1}^{3.8}$	0.6 ± 0.1	5 ± 1	2.5 ± 0.5	4.0 (5.8 ^c)	2.4 (4.1 ^c)
Feb 18, 05	36.8	33	0.8 ± 0.1	—	$0.52 \pm_{0.10}^{0.07}$	—	$24 \pm_{8}^{12}$	—	2.2 (23.7 ^c)
Feb 18, 05	41.6	32	0.19 ^b	$2.5 \pm_{0.8}^{2.8}$	0.6 ± 0.1	5 ± 1	$2.0 \pm_{0.2}^{0.7}$	—	2.2 (3.8 ^c)
Sep 08, 05	6.2	4	$< 0.9^d$	—	$1.0 \pm_{0.6}^{1.1}$	—	$< 12^e$	—	0.6 (1.1 ^c)

Notes to the Table:

- a - The emission measure (EM) is derived, for each temperature component, from the fit parameter K, through the relationship $EM = K \times 10^{14} 4\pi d^2$, where d is the source's distance (in cm)
- b - frozen parameter
- c - unabsorbed flux
- d - the best fit value corresponds to $N_H = 0.4 \cdot 10^{22} \text{ cm}^{-2}$
- e - the best fit value corresponds to $EM = 2.5 \cdot 10^{52} \text{ cm}^{-3}$
- the quoted errors correspond to a 90% confidence level

timing with an optical-IR post-outburst phase, if not completely fortuitous, can support a direct connection: a sort of modulation over the coronal mechanism which tends to reduce the X-ray emission. Indeed, according to Preibisch et al. (2005), the accretion events do reduce the X-ray activity; we can only say that this effect cannot be explained as due to intervening extinction, but to some other effects (e.g. a weaker dynamo action related to the magnetic disk locking).

4. The emerging picture and concluding remarks

In this section we summarize the results presented above trying to delineate a coherent picture for V1118 Ori. Firstly, in Table 6 the relevant information derived in the present work is listed along few literature data.

V1118 Ori appears to be an accreting young object which undergoes quasi periodic outbursts whose monitoring, so far conducted only in the visual band has been started also in the near IR and X-ray bands. The first marginal detection in the mid-IR (near 8 μm) is also provided. Our observations largely confirm its EXor nature: its bolometric luminosity increases from $1.4 L_{\odot}$ to more than $25 L_{\odot}$ passing from inactive to active phases.

V1118 Ori presents a SED typical of an accreting T Tauri star and also its near-IR spectrum strictly resembles that of T Tauri, showing strong H I, He I and CO features in

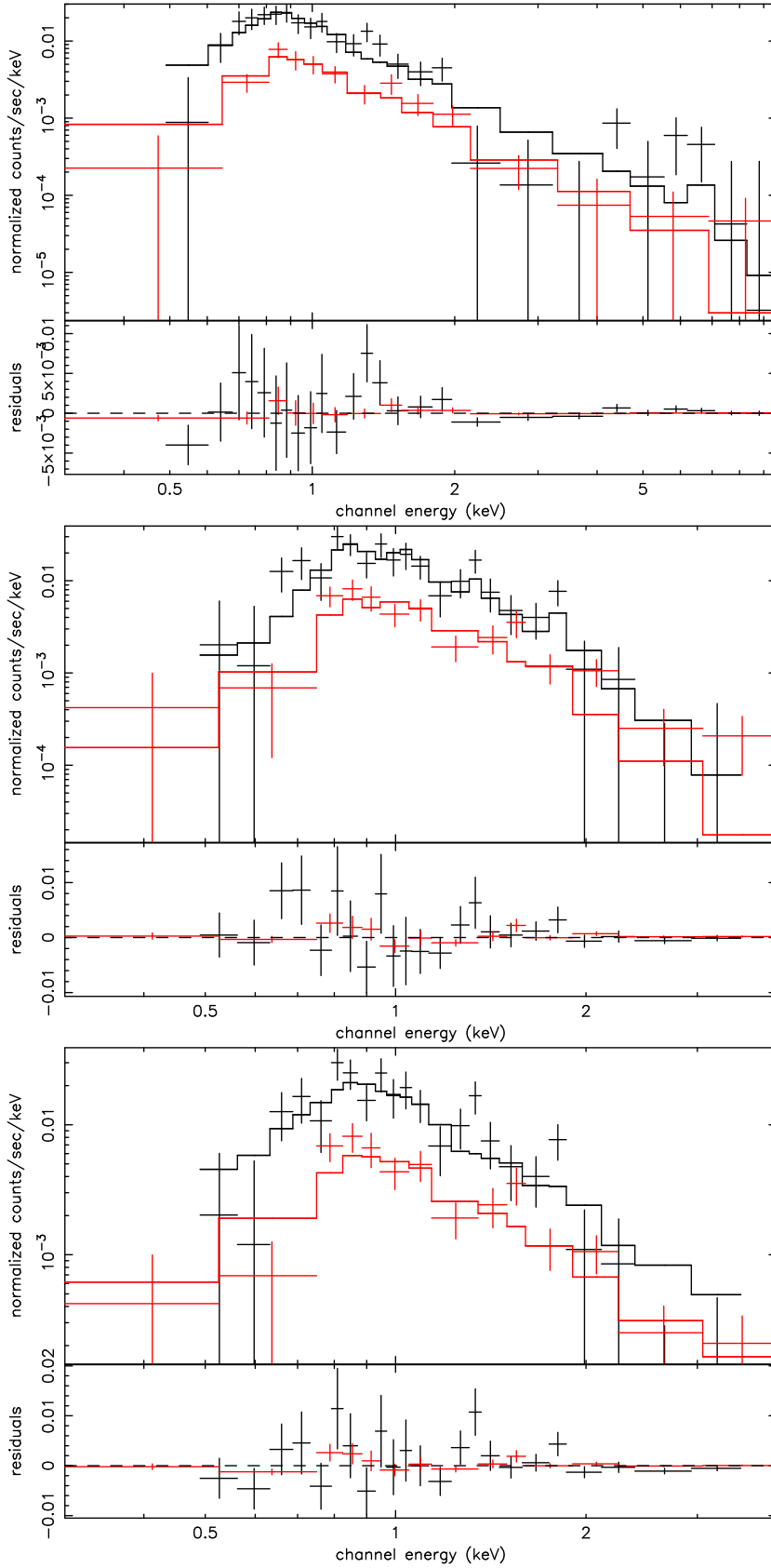


Fig. 5. *Top panel:* X-ray spectrum (0.5 - 10 keV - February 2005) of V1118 Ori observed with the EPIC PN and MOS detectors on board XMM. A double-temperature thermal model has been adopted to fit the data (see text). The residuals computed in each bin are reported as well. *Middle panel:* as above, where the 0.5 - 3.5 keV portion is fitted with a single temperature model. *Bottom panel:* as above, where the 0.5 - 3.5 keV portion is fitted with a double temperature model.

Table 6. V1118 Ori derived parameters.

Parameter ^a		Value
Distance	d	460 pc
Spectral Type		M1e
Stellar radius	R _*	1.29 R _⊙
Bolometric luminosity	L _{bol}	1.4 L _⊙ (min) > 25.4 L _⊙ (max)
X-ray luminosity	L _X (0.5-3.5 keV)	0.6-2.2 10 ⁻⁴ L _⊙
Plasma temperature	T	7 - 11 10 ⁶ K
Visual extinction	A _V	0 - 2 mag
Wind velocity	v _w	200 km s ⁻¹
Mass loss rate	\dot{M}	4 ± 2 10 ⁻⁸ M _⊙ yr ⁻¹ (ionized) 3-8 10 ⁻⁷ M _⊙ yr ⁻¹ (neutral)
Ionization fraction		0.1 - 0.2
Envelope size		8 ₋₂ ⁺⁴ R _*

Note to the Table:

a - The first three lines of the table list literature parameters, while the remaining are derived in the present work.

emission. The near-IR colors do not seem to undergo extinction variations and are always compatible with low A_V values (0-2 mag). Beside the accretion disk, the star has a quite compact and partially ionized circumstellar envelope created by the mass loss in stellar winds which are likely accretion-generated. V1118 Ori is presumably in a late stage of its pre-main sequence evolution and this is likely the reason of its unobscured appearance. The lack of any collimated outflow driven by the source provides further support to this hypothesis. Large part of the relevant physics of V1118 Ori originates in its accretion disk. By studying its X-ray properties, a coronal origin is confirmed as the responsible for the high energy emission with some influence by accretion. The parameters derived by X-ray observations (plasma temperature and ratio L_X/L_{bol}) are all in agreement with those obtained for active T Tauri stars.

All the observational evidences presented in this paper show the similarity of V1118 Ori with low luminosity unobscured T Tauri stars: this behaviour suggests that: (i) the EXor evolutionary stage appears to follow the FUor one, more likely than to be a less evident manifestation of the same phase; and (ii) the scanty number of known EXor could be simply due to the difficulty of performing an accurate multi-frequency monitoring of all the active T Tauri stars.

We will continue our IR monitoring program by extending the investigation also to shorter timescales (hours, days). Indeed significant clues of rapid variations are already presented here (Sect. 3.1), but wide databases have to be accumulated to properly study to what extent the accretion processes are dynamical on several timescales.

Acknowledgements. The authors would like to thank the referee Marc Audard for his constructive comments on different aspects of this paper.

References

- Audard, M., Güdel, M., Skinner, S.L. et al. 2005 ApJ 635, L81
- Carr, J.S. 1989 ApJ 345, 522
- Chanal, M. 1983 IAUC n.3763
- Cutri, R.M., Strutskie, M.F., Van Dyk, S. et al. 2003 Explanatory Supplement to the 2MASS All Sky Data Release (Pasadena: Caltech)
- D'Alessio, F., et al. 2000 Proc. of the SPIE Symp. on *Astronomical Telescopes and Instrumentation*, eds. M. Iye & A.F.M. Moorwood, 4008, 748
- D'Alessio, P., Calvet, N., Hartmann, L., Lizano, S. & Cantó, J. 1999 ApJ 527, 893
- Di Paola, A., Lorenzetti, D., Calzoletti, L. et al. 2005 ATel 619
- Esteban, C., Peimbert, M., Torres-Peimbert, S. & Escalante, V. 1998 MNRAS 298, 185
- Feigelson, E.D. & Montmerle, T. 1999 Ann. Rev. Astron. Astrophys. 37, 363
- García García, J., Mampaso, A. & Parsamian, E.S. 1995 *Information Bulletin of Variable Stars* n.4268
- García García, J. & Parsamian, E.S. 2000 *Information Bulletin of Variable Stars* n.4925
- Gasparian, L.G., Melkonian, A.S., Ohanian, G.B. & Parsamian, E.S. 1990 *Flare Stars in Star Clusters, Associations, and the Solar Vicinity* Proc. 137th Symposium of the International Astronomical Union, Byurakan [Armenia], U.S.S.R., October 23-27, 1989. Editors, L.V. Mirzoyan, B.R. Pettersen, & M.K. Tsvetkov; Publ. Kluwer Academic, Dordrecht, The Netherlands, Boston, MA.
- Greene, T.P. & Lada, C.J. 1996 AJ 112, 2184
- Grosso, N., Kastner, J.H., Ozawa, H. et al. 2005 A&A 438, 159
- Hartmann, L., Hinkle, K. & Calvet, N. 2004 ApJ 609, 906
- Hartmann, L., Kenyon, S. & Hartigan, P. 2003 *Protostars and Planets III*, eds. E.H. Levy & J.I. Lunine, p.497
- Hayakawa, T., Ueda, T., Uemura, M. et al. 1998 *Information Bulletin of Variable Stars* n.4615
- Herbig, G.H. 1977 ApJ 217, 693
- Herbig, G.H. 1989 Proc. of the ESO Workshop on *Low Mass Star Formation and Pre-Main Sequence Objects*, ed. B. Reipurth, p.233
- Hillenbrand, L.A., Strom, S.E., Calvet, N. et al. 1998 AJ 620, L107

- Jansen, F., Lumb, D., Altieri, B. et al. 2001 A&A 365, L1
- Kastner, J.H., Huenemoerder, D.P., Schultz, N.S. et al. 2004a ApJ 605, L49
- Kastner, J.H., Richmond, M., Grosso, N. et al. 2004b Nature 430, 429
- Kóspál, Á., Ábrahám, P. & Csizmadia, Sz. 2004 Baltic Astronomy 13, 518
- Meyer, M.R., Calvet, N. & Hillenbrand, L.A. 1997 AJ 114, 288
- Mewe, R., Kaastra, J.S. & Liedahl, D.A. 1995 Legacy, 6, 16,
<http://heasarc.gsfc.nasa.gov/docs/journal/meka6.html>
- Muzerolle, J., Megeath, S.T., Flaherty, K.M. et al. 2005 ApJ 116, 1816
- Nisini, B., Antonucci, S. & Giannini, T. 2004 A&A 421, 187
- Parsamian, E.S. & Gasparian, K.G. 1987 Astrophysics 27, 598
- Parsamian, E.S., Ibragimov, M.A., Ohanian, G.B. & Gasparian, K.G. 1993 Astrophysics 36, 23
- Paul, C., Kroll, P. & Lehmann, T. 1995 Lecture Notes in Phys. 151, 229
- Preibisch, T., Kim, Y-C., Favata, F. et al. 2005 ApJ in press
- Reipurth, B. & Aspin, C. 1997 AJ 114, 2700
- Reipurth, B. & Aspin, C. 2004 ApJ 606, L119
- Rieke, G.H. & Lebofsky, M.J. 1985 ApJ 288, 618
- Scoville, N.Z., Krotkov, R. & Wang, D. 1980 ApJ 240, 929
- Stanke, T., McCaughrean, M.J. & Zinnecker, H. 2002 A&A 392, 239
- Strüder, L., Briel, U., Dennerl, K. et al. 2001 A&A 365, L18
- Turner, M.J.L., Abbey, A., Arnaud, M. et al. 2001 A&A 365, L27
- Vacca, W.D., Cushing, M.C. & Simon, T. 2004 ApJ 609, L29
- Williams, P. & Heathcote, N.S.W. 2005 IAUC n.8460